International Journal of Bridge Engineering (IJBE), Special Issue 2017, pp. 79-97

DESIGN OF ISOLATED BRIDGES FOR MULTI-LEVEL SEISMIC PERFORMANCE USING GAPPED DEVICE CONNECTIONS

Murat Dicleli[1] and Ali Salem Milani[2]

[1,2] Middle East Technical University, Ankara, Turkey
e-mail: mdicleli@metu.edu.tr

ABSTRACT: Hysteretic dampers in bridges with seismically isolated decks are coupled with shock transmitters in order to prevent their engagement during thermal displacements of the deck. An alternative design approach is presented in this paper where the dampers are attached to the deck using elongated holes (gaps) which are sized to accommodate the thermal displacements and hence to keep the dampers from being activated during thermal displacements. The gaps are sized based on the expected maximum thermal displacement in each pier. The gap length will thus be different for different piers. With this arrangement, number of the dampers engaged during an earthquake will depend on the magnitude of displacements. The distinct feature in this design is: (i) preventing the engagement of dampers under thermal displacements during service life without using shock transmitters and (ii) sequential engagement of dampers as a function of magnitude of seismically-induced displacements. This paper presents a sample application of this methodology in design of a major viaduct. The performance goals of the bridge require no damage at 475-year return period earthquake and repairable damage at 2475-year return period earthquake. The bridge is designed with a seismic isolation system composed of spherical bearings and hysteretic dampers (Multidirectional torsional hysteretic damper (MTHD)). Design features of this seismically isolated bridge and results of nonlinear time-history analyses are presented in this paper.

KEYWORDS: isolated bridge; isolation; damper; performance-based design; time-history; damage index.

1 INTRODUCTION

Special seismic protection, usually in the form of isolation or energy dissipation devices or combination of both, is often required for seismic protection of important structures located in areas of high risk of seismic activity to satisfy design objectives of controlled structural response and minimal or no damage. For structures subjected to earthquakes with intense long duration acceleration pulses, although seismic isolation technology may be used to reduce and control

the magnitude of the forces, such a system alone may not be adequate to reduce the displacement demand to practical ranges of application [1]. In such cases, a combination of seismic isolation and energy dissipation devices or dampers is used to reduce and control both forces and displacements. Use of seismic isolation combined with energy dissipaters in bridges is as widespread. This paper is meant to be a demonstration of application of modern seismic isolation techniques to achieve a performance-based design of a bridge.

2 DESCRIPTION OF THE BRIDGE, CONSTRUCTION SITE AND KEY ANALYSIS AND DESIGN CRITERIA OF SEISMIC ISOLATION

Fig. 1 shows the satellite view and a perspective view of the Bitlis River Viaduct. The viaduct spans the Bitlis River in eastern Turkey with a total length of 1390 meters. Part of this bridge with a length of 801 meters containing 17 spans is designed as a post-tensioned box girder bridge, 19.6 meter width and girder depth of 3.0 meters, which is to be constructed using the incremental launching method. The height of the piers in this part of the bridge vary between 14 to 37 meters. Elevation view and a typical cross section of the bridge and the deck are shown in Fig. 2.

Isolation system of the bridge is composed of spherical bearings coupled with steel hysteretic dampers with re-centering capability; MTHD (Multidirectional Torsional Hysteretic Damper). The targeted seismic performance is defined as no damage in DBE and repairable damage in MCE. This is achieved using gapped connections for dampers, using elongated holes, to allow for sequential engagement of dampers as a function of magnitude of seismically-induced displacements. Use of gaps to achieve multi-level performance goals has also been proposed in case of isolated buildings, where gapped connections are used to defer the engagement of dampers in low-intensity seismic events [2],[3]. The gaps provided in connection of dampers to deck serve the simultaneous purpose of accommodating the thermal displacements such that the dampers are not activated due to thermal displacements. The gaps are sized based on the expected maximum thermal displacement in each pier, being different for different piers. With this arrangement, the objective of controlling the number of the dampers engaged during an earthquake based on the magnitude of displacements, is achieved.

The initial design of the isolated bridge is performed using equivalent linear analysis to estimate the displacement demand on isolators and the base shear in substructure, followed by nonlinear time-history response analysis of the 3D model of the bridge. Realization of performance goals is established by calculation of damage indices and comparison with the proposed limits in accordance with the expected performance level.

3 SEISMICITY OF THE SITE AND SEISMIC PERFORMANCE GOALS

Fig. 3 shows the site seismicity and the site-specific design spectrum, as obtained from a probabilistic seismic hazard analysis [4]. The site is located in a seismically active zone where seven potential sources of seismic activity were identified, two of which are capable of producing earthquakes with maximum magnitude of 7.6. The performance goals set for this viaduct are defined as follows:

• For 72-year return period earthquake (i.e., during construction): No damage
• For 475-year return period earthquake (design-basis earthquake): No damage
• For 2475-year return period earthquake (maximum considered earthquake): Repairable damage.

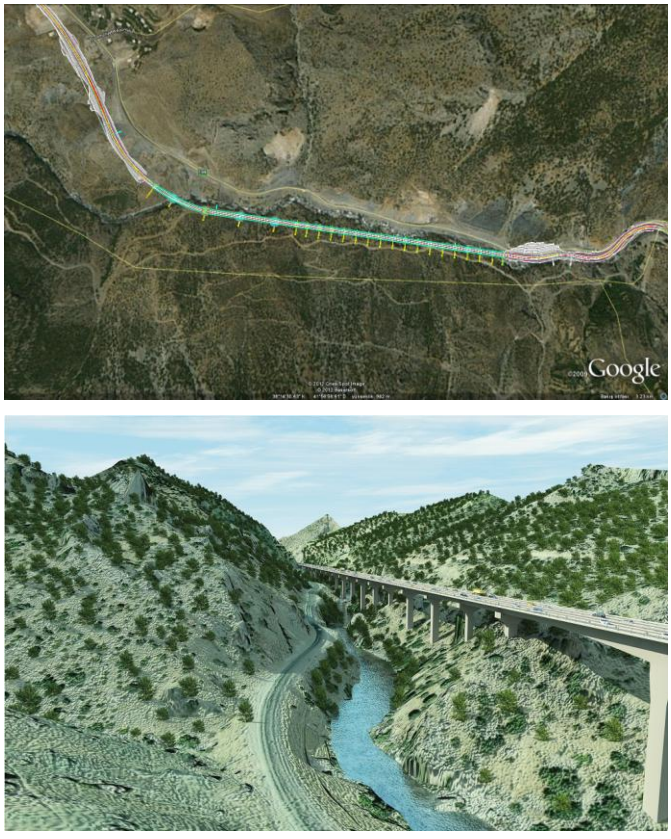

Figure 1. Satellite and perspective views of the viaduct

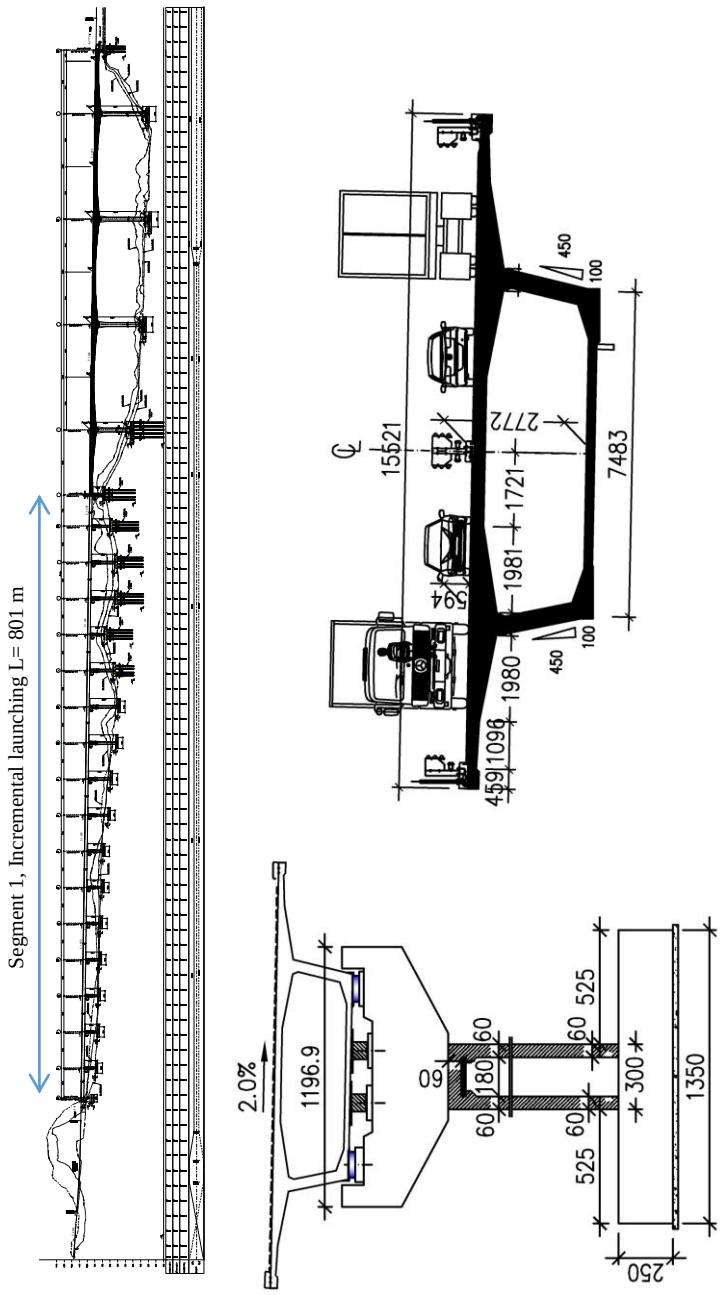

Figure 2. Elevation and cross-section views of the bridge and the deck

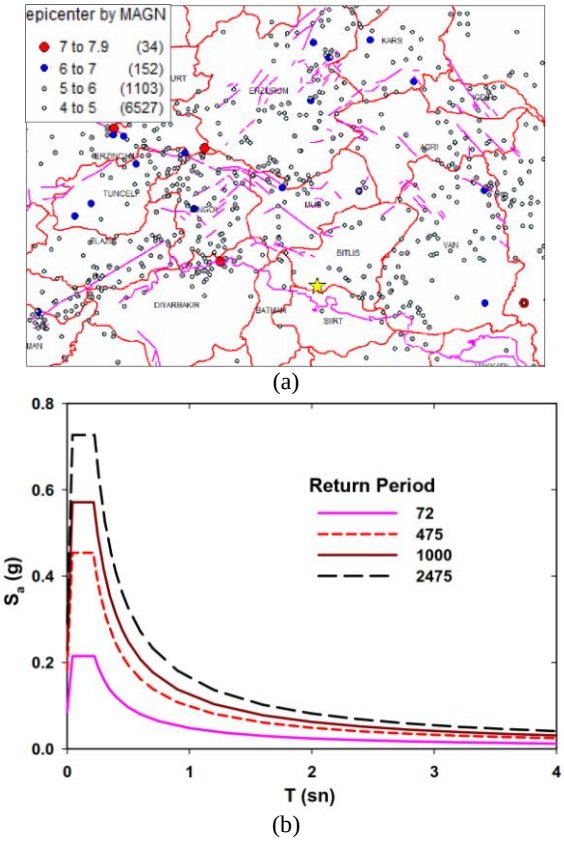

(a)

(b)

Figure 3. (a) Site seismicity (the site is shown by a yellow star); (b) Site-specific design spectrum

4 SEISMIC ISOLATION SYSTEM SELECTED FOR DESIGN

The viaduct is located in a very cold area where the temperature can reach -22^{o}C, a seismic isolation system that performs reliably in cold temperatures is needed. Accordingly, spherical bearings coupled with steel hysteretic dampers with re-centering capability; MTHD (Multidirectional Torsional Hysteretic Damper) are chosen. A brief description of the newly-developed MTHD damper is given in the following. MTHD is designed to dissipate energy through yielding and plasticization of cylindrical energy dissipaters under torsion. Eight of these identical energy dissipaters each attached to a torsion arm are arranged in a symmetric configuration to create the MTHD. Fig 4(a) and (b) show perspective and side views of MTHD, respectively. Fig. 4(c) shows a section view of MTHD with a typical energy dissipation unit of MTHD. All of the parts which compose the damper are named in Fig 4(a) and Fig 4(c). However, for the sake of brevity, detailed description of the device is not given here and the interested reader is referred to reference [3]. To convert translational motion of the structure to twisting in the cylindrical energy

dissipaters, each arm is coupled with a guiding rail which through a low-friction slider block guides the motion of the arm. Schematic top-views of MTHD at un-displaced and displaced positions are shown in Fig. 4(d).

A distinguishing feature in force-displacement response of MTHD is the geometric hardening behavior which is the outcome of translation-to-rotation motion conversion mechanism in the energy dissipation units of MTHD, as schematized in Fig. 5(a). This mechanism, magnifies the reaction force required to balance the torque in energy dissipaters. Fig. 5(a) shows a typical energy dissipation unit with arm length L, subjected to displacements d_1 and d_2, where $d_2>d_1$. Let the rotation angle of the arm, the reaction force and the torque are denoted by θ, f and T, respectively and let the numerical index indicate the corresponding state of displacement. Given that $T=f.L.\cos\theta$, and since increasing displacement leads to reduction in $\cos\theta$ without any reduction in T, it can be easily shown the $f_2>f_1$, that is:

$$\frac{T_2}{L\cos\theta_2} > \frac{T_1}{L\cos\theta_1} \Rightarrow f_2 > f_1 \tag{1}$$

Note that the reaction force of the device is the sum of projections of all eight forces coming from eight energy dissipation units. Thus, the hardening behavior at eight energy dissipation units directly leads to similar behavior in global response of the device. The described mechanism also offers the possibility of controlling the desired level of hardening in force-displacement response, through adjustment of the arm length to maximum displacement ratio. Varying levels of hardening obtained as such, leads to hysteresis loops of different shapes as shown in Fig. 5(b). As indicated on these graphs, the parameter used to characterize hardening in the MTHD is named 'Hardening Index', defined as;

$$HI = \frac{F_{max}}{F_Y} \tag{2}$$

where F_{max} and F_Y stand for maximum force capacity (force at D_{max}) and effective yield force of MTHD. A 200kN, 120mm-capacity version of the device was built and tested in UniBw/Munich and also at METU/Ankara. The sketch and photo of the test setup are shown in Fig. 6(a),(b). Fig. 6(c) shows the instrumentation scheme. Fig. 6(d),(e),(f) show the MTHD under test at METU/Ankara at un-displaced position and two extreme strokes of ±120mm, respectively. Force-displacement response loops of MTHD, as obtained from tests are given in Figs. 7(a),(b), which depict a very stable cyclic response with little variation in force levels not exceeding 4.0% the mean value. MTHD is capable of reaching high force and displacement capacities, shows high levels of damping, controllable post-elastic stiffness and very stable cyclic response. A design methodology for the device has also been completed. Further details on this device can be found in [6],[7].

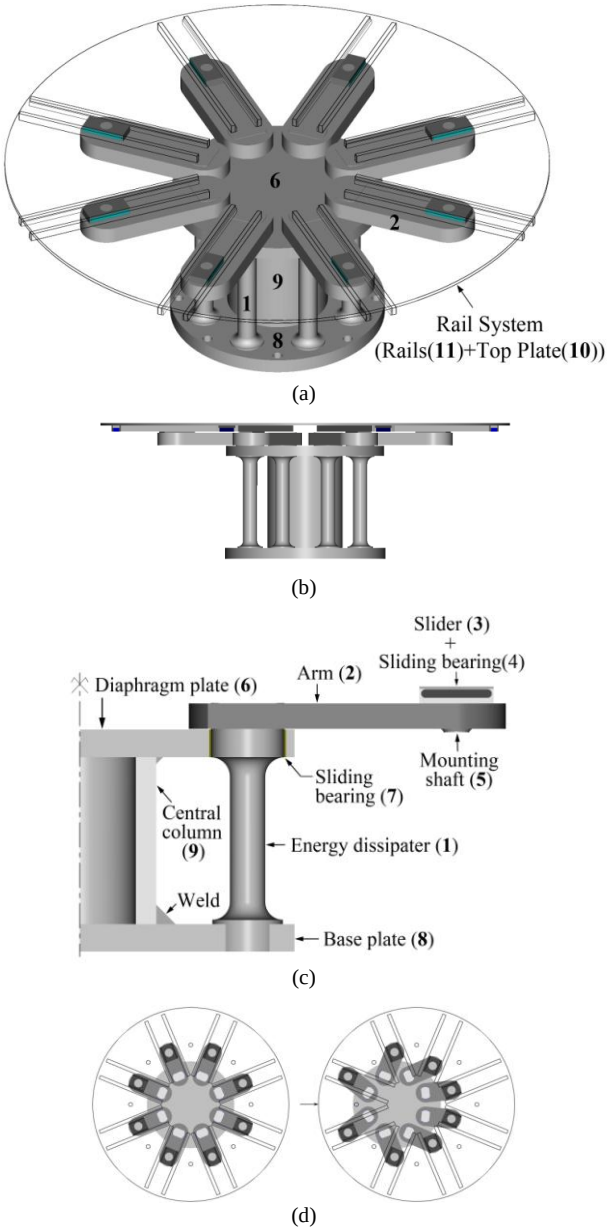

Figure 4. Multidirectional Torsional Hysteretic Damper (MTHD): (a) Isometric view showing the rail system and base device underneath; (b) side view; (c) Section view showing a single energy dissipation unit of MTHD; (d) Schematic top-view of MTHD at un-displaced and displaced positions

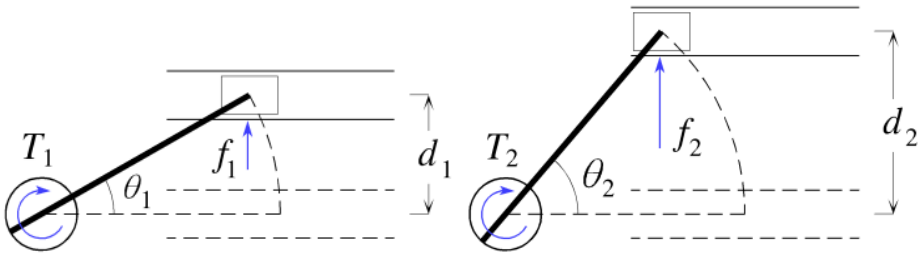

(a)

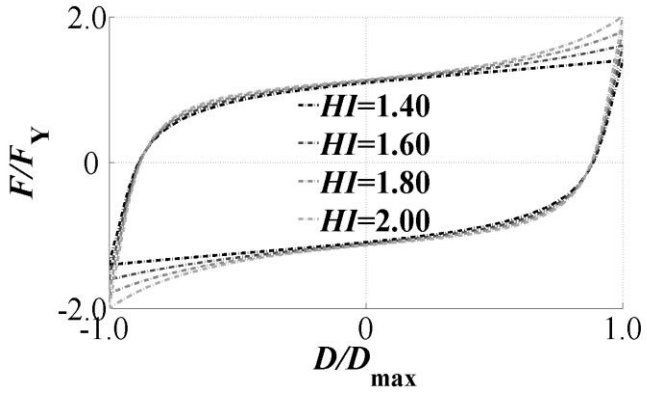

(b)

Figure 5. (a) Working mechanism of MTHD responsible for geometric hardening; (b) MTHD response for different design hardening indices

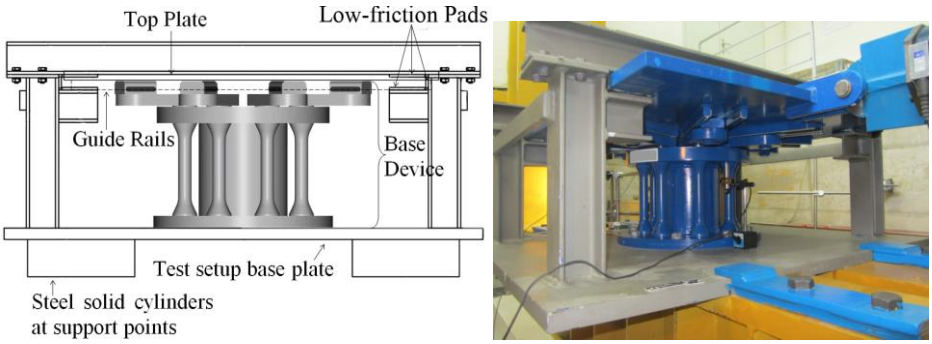

(a) (b)

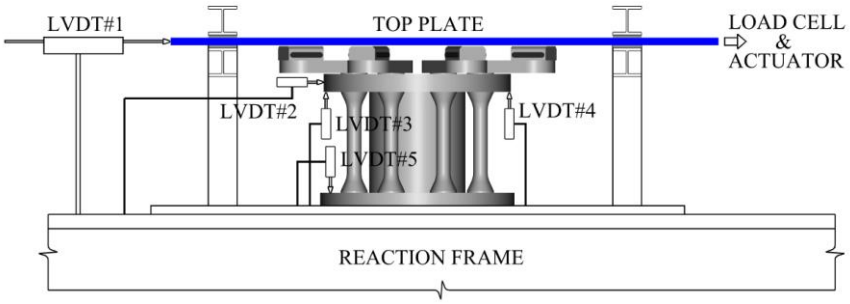

(c)

(d) (e) (f)

Figure 6. 200*kN*, 120*mm*-capacity prototype MTHD: (a) Schematic side view of the test setup; (b) perspective view of the test setup; (c) instrumentation scheme; MTHD under test at: (d) un-displaced position, (e),(f) two extreme strokes of ±120*mm*

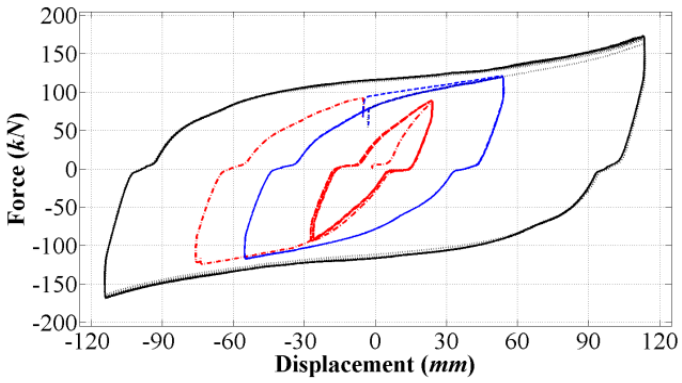

(a)

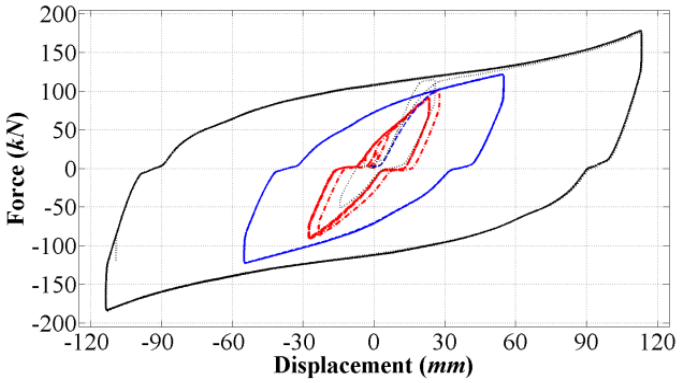

(b)

Figure 7. Cyclic response of prototype MTHD, obtained from tests of MTHD with energy dissipaters made of: (a) S355J2+N, (b) C45 steel grades

5 THE ISOLATION SCHEME OF THE BRIDGE

Fig. 8 shows a schematics of the isolation of the part of the bridge located between the abutment A1 and pier P17. The part of the bridge between P17 and the abutment A2 is built using balanced cantilever method where the piers are built monolithically with the deck. The expansion joints are located on two abutments and pier P17. The focus in this study is the part of the bridge between the abutment A1 and pier P17. As shown in Fig. 8, the spherical bearing on the abutment A1, pier P17 and three additional piers on each side are unidirectional to resist wind loads. That is, at these points the bridge is fixed to the abutment/pier in the transverse direction. On the 10 piers in between, the spherical bearings are multidirectional and the bridge is free to move both laterally and longitudinally during an earthquake. Under wind loads, the

dampers provide the required resistance in the transverse direction within their elastic limit. The MTHDs are placed on these 10 piers, two on each pier, as shown in the cross-section view in Fig. 9(a). An issue to be tackled with the use of the hysteretic dampers is the presence of thermal movements in certain piers. The bridge is designed to eliminate the thermal movements at its two abutments where the expansion joints are located. That is, thermal action expands or contracts the deck from the middle. Therefore, the dampers on piers away from the middle pier(s) will be subjected to thermal displacements, the intensity of which depends on the pier's distance from the middle point of the deck. To prevent the low-cycle fatigue in dampers as a results of repeated thermal displacements, the attachment of the dampers to the deck is designed to be via elongated holes (slots), as shown in Fig. 9(b). This way, a gap is left between the anchorage and the upper plate of the MTHD, in the longitudinal direction of the bridge. The gap is sized to accommodate the maximum probable thermal displacement per each pier. The amount of gap provided for MTHDs on each pier is indicated in Fig. 8. An alternative solution would be to use shock transmission units (luck-up devices) to connect the dampers to the deck. However, this solution entails increased cost and reduced reliability since shock transmission units are both expensive and require maintenance. The design of the MTHDs with gaps, as described above, was also meant to serve a second objective. Presence of gaps in connections of certain MTHDs means that the engagement of these dampers during an earthquake depends on whether the intensity of the displacements are large enough for the gaps to close. That is, at very low-intensity events, only dampers on middle piers (P8 and P9) are engaged; thus, preventing both the unnecessary increase in base shear on the other piers and also damage to the MTHDs on those piers. With increasing intensity of the ground motion more number of MTHDs on piers come into action. This sequential engagement of the dampers is the performance-based oriented feature in this design. In addition the dampers, which are connected without slots on Piers 8 and 9 provide the required resistance within their elastic range against breaking forces.

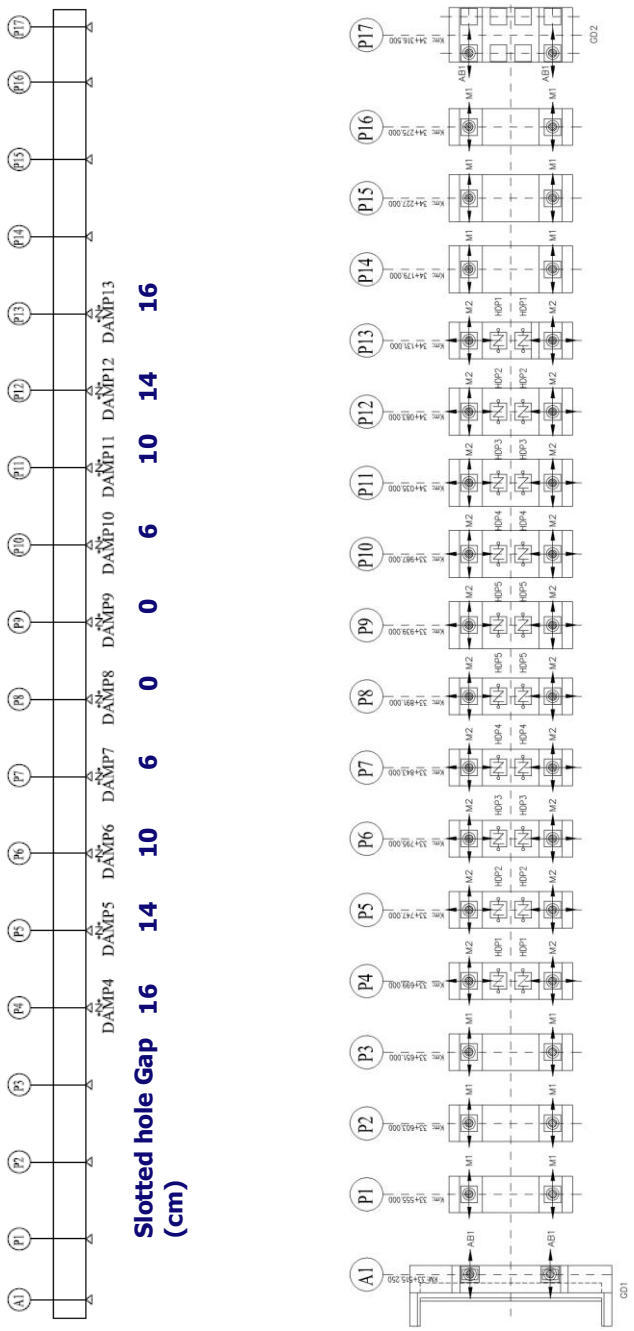

Figure 8. Schematics of the isolation system

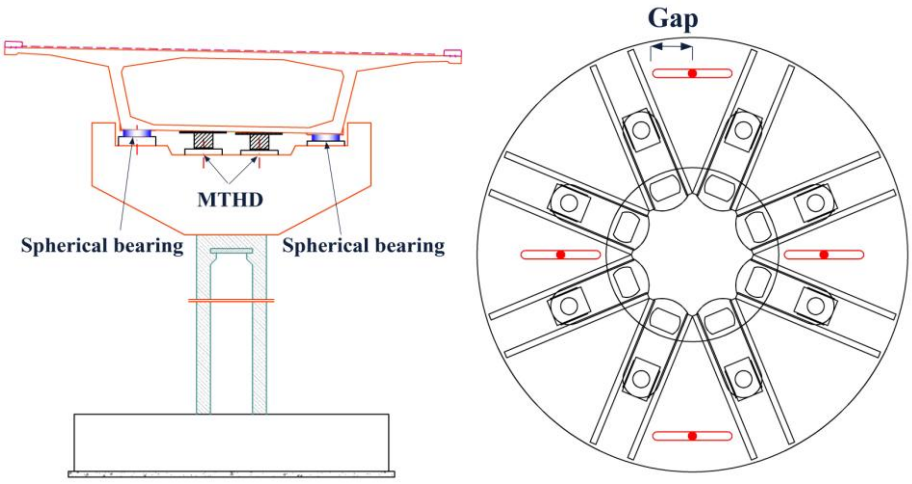

(a) (b)

Figure 9. (a) Installation of two MTHDs on a typical pier; (b) The provided gaps (longitudinal direction) on the upper plate of the MTHDs where the device is mounted to the deck

6 SEISMIC PERFORMANCE CRITERIA FOR THE MTHD-EQUIPPED VIADUCT

Based on the arrangement of the MTHDs, as laid out in previous section, the seismic performance goals of no damage at DBE and repairable damage in MCE are redefined as follows: at DBE (475 years return period), limited number of dampers (those with zero and 6 cm slot gaps) will be engaged during the earthquake in the longitudinal direction. No damage will be inflicted in the substructure members. If needed, energy dissipaters of few dampers could be replaced after the earthquake. At MCE (2475 years return period), dampers with larger slot gaps will also be engaged sequentially as the intensity of the ground shaking increases. The central piers may yield after the damper reach a certain force level. In the preliminary design stage, equivalent linear analysis method was used to determine the required surface coefficient of the spherical bearings and force/displacement capacity of the MTHDs. In equivalent linear analyses, energy dissipated by the MTHDs is accounted for through the effective damping coefficient, β_{eff} , defined as [5]:

$$\beta_{eff} = \frac{1}{2\pi} \frac{W_D}{K_e \cdot U_{\max}^2} \tag{3}$$

Where, W_D is the hysteretic energy dissipated per cycle, U_{max} denotes the maximum cyclic displacement and K_e is the effective stiffness, defined as the secant stiffness at U_{max}. Thus, to perform the equivalent linear analyses, requires calculation of hysteretic energy dissipated per cycle of MTHD, i.e., area under

the hysteresis loop, either using a subroutine or a simplified equation. Despite that the shape of hysteresis loop of MTHD is not bilinear, it is shown that simplified equations can be developed to calculate the effective damping coefficient at the desired displacement, for any MTHD with a certain hardening index (*HI*) and produced using any specific steel [6].

Following the initial design, a series of time-history response analyses are performed to assess whether the proposed design meets the performance objectives. The results are presented in the following section.

7 TIME-HISTORY RESPONSE ANALYSES

To assess the performance of the bridge in DBE and MCE-level earthquakes, a 3D model of the bridge was built in SAP2000, as shown in Fig. 10(a). Spherical bearings are modelled using rigid plastic model (using nonlinear link element with Wen plasticity model where the elastic stiffness is taken very high) and the MTHD dampers are modelled using nonlinear links with multi-linear kinematic hardening behavior and force-displacement curve plotted in Fig. 10(b). The effect of soil-structure interaction was found to be negligible due to the stiff soil condition under the foundations. The model is subjected to seven bi-directional design spectrum-compatible ground motions, as specified in Table 1. These ground motions are proposed as part of a site-specific study and are compatible with the seismicity of the site [4]. The analyses were performed in both orthogonal directions separately. As the bridge is seismic isolated, the forces transferred to substructure and other components are limited and controlled. Therefore, severe deformation and cracking is not expected in the structure. Accordingly, neither the shear effect nor the effect of structural damping are expected to be significant.

Displacement response histories of the MTHD dampers in the longitudinal direction for Kocaeli and Landers records (two records with the largest magnitude) for both MCE and DBE events are presented in Fig. 11. Sample hysteresis loops of damper on piers No. 6 and 9 in the longitudinal direction for Kocaeli record are given in Fig. 12. The maximum displacement of the MTHDs in the longitudinal directional was found to be 330mm. The dampers were thus designed for a displacement capacity of 350mm. The displacement in the transverse direction of the bridge was found to be small and did not govern the design displacement of the damper.

Table 1. Specification of the design spectrum-compatible ground motions.

No.	Event	M_w	Fault Type	Station	Scale Factor		
					%10/50yr	%5/50yr	%2/50yr
1	Imperial Valley, 1979	6.5	Strike Slip	6604 Cerro Prieto	1.00	1.25	1.40
2	Landers, 1992	7.3	Strike Slip	21081 Amboy	0.75	0.85	0.90
3	Kocaeli, 1999	7.4	Strike Slip	Gebze	0.75	0.90	1.00
4	Duzce, 1999	7.1	Strike Slip	531 Lamont	1.40	1.70	1.90
5	Nahanni, 19856	6.8	Reverse Oblique	6099 Site 3	0.75	0.95	1.10
6	Spitak, 1988	6.8	Reverse Oblique	12 Gukasian	0.90	1.20	1.40
7	Loma Prieta, 1989	6.9	Reverse Oblique	58378 APEEL 7	1.00	1.15	1.25

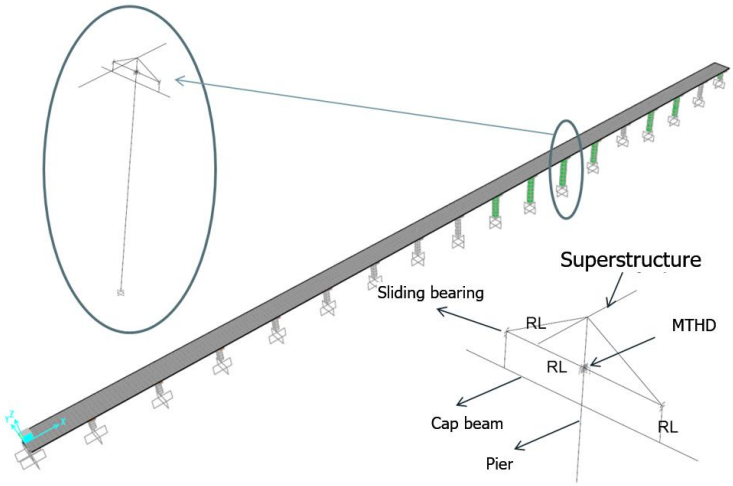

(a)

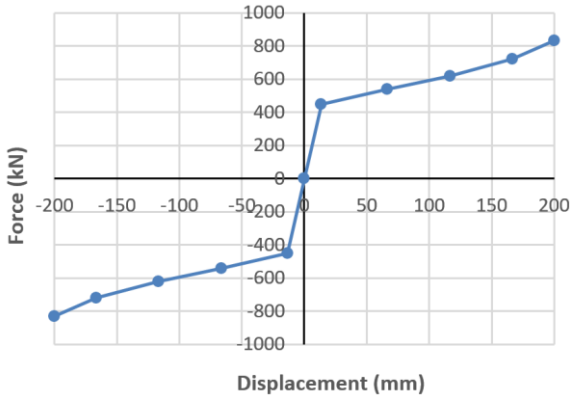

(b)

Figure 10. (a) Structural model of the bridge; (b) Multilinear force-displacement curve of MTHD

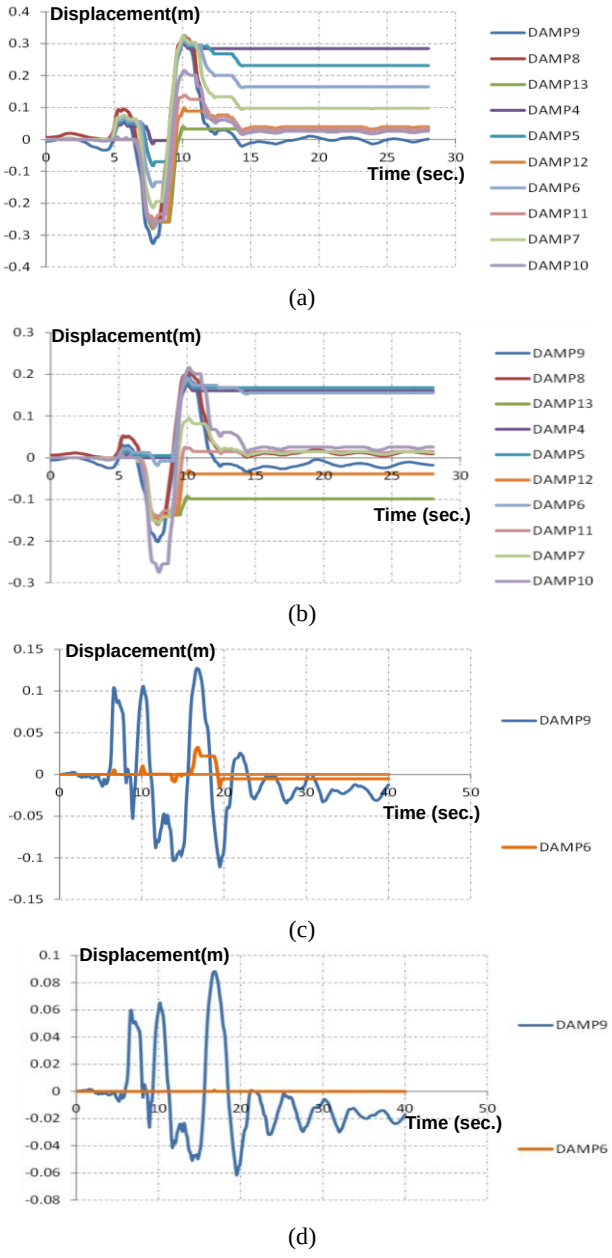

Figure 11. Displacement response time history of the dampers in the longitudinal direction for (a) Kocaeli MCE; (b) Kocaeli DBE; (c) Landers MCE and (d) Landers DBE, earthquake records

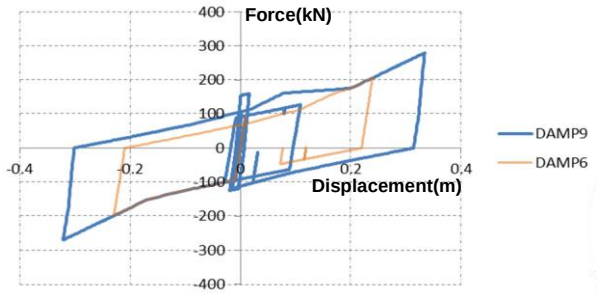

(a)

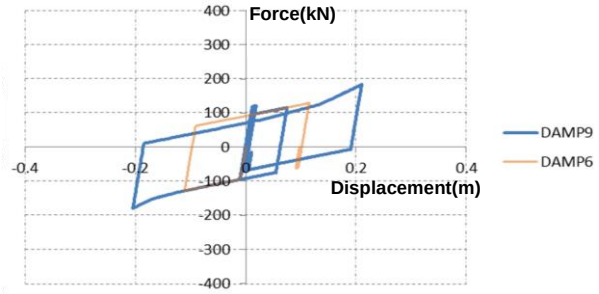

(b)

Figure 12. Sample hysteresis loops of damper on piers No. 6 and 9 in the longitudinal direction for (a) Kocaeli, MCE and (b) Kocaeli, DBE records

8 DAMAGE ANALYSIS

To evaluate the performance of the bridge, the state of damage in the piers should be assessed. The damage Model of Hindi and Sexsmith [8] is used for this purpose. The damage model takes as a reference the monotonic energy dissipation capacity of a structure in the undamaged virgin state, which is defined as the area, A_o, under the static pushover curve up to the point of failure (Fig. 13(a)). With the actual "n" cycles of load-displacement history applied on the structure due to a potential earthquake, the remaining monotonic energy dissipation capacity of the structure, compared to that in its virgin state, defines the extent of damage. The remaining monotonic energy dissipation capacity of the structure is defined as the area, A_n, under the static pushover curve obtained from the end of the last cycle, n, to the failure point (Fig. 13(b)). Accordingly, the damage index is the ratio:

$$DI_n = \frac{A_o - A_n}{A_o} \tag{4}$$

A damage index of 0.0 (A_n=A_o) is indicative of no damage, whereas a damage index of 1.0 (A_n=0) is indicative of complete damage or collapse. The damage index is correlated with the physical state of damage, according to the following scale:

- DI<0.2: Minor damage–light cracking–very easy to repair.
- 0.2≤DI<0.4: Moderate damage–severe cracking, cover spalling–repairable.
- 0.4≤DI<0.6: Severe damage-extensive cracking, reinforcement exposed–repairable with difficulties.
- 0.6≤DI<1.0: Severe damage–concrete crushing, reinforcement buckling–irreparable.
- DI=1.0: Complete collapse.

The calculated damage indices are given in Table 2. For DBE-level earthquakes, the DI values are all below 0.2, indicating that the objective of no damage at DBE is met. Likewise, in case of MCE-level earthquakes, all DI values fall below 0.4 indicating that the objective of repairable damage at MCE is met. It should be emphasized that these conclusions are drawn in the framework of the proposed damage model and the proposed correlation between the damage index defined by Hindi and Sexsmith [8] and the expected physical state of damage (an alternative to a fragility function).

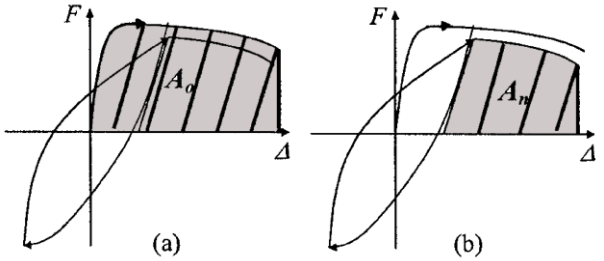

Figure 13. Definition of damage equation parameters of the model by Hindi and Seximith [8]: (a) monotonic energy in the virgin state; (b) monotonic energy after the application of load-displacement cycles

Table 2. Calculated damage indices.

Earthquake	Imperial Valley, 1979	Landers, 1992	Kocaeli, 1999	Duzce, 1999	Nahanni, 1985	Spitak, 1988	Loma Prieta, 1989	Average
DBE	0.06	0.09	0.12	0.10	0.03	0.05	0.08	0.076
MCE	0.11	0.19	0.27	0.21	0.07	0.13	0.22	0.171

9 CONCLUSIONS

The paper presents a practical application of seismic isolation technique following a performance-based design approach for a bridge. The bridge is designed with a seismic isolation system composed of spherical bearings and Multidirectional Torsional Hysteretic Damper (MTHD). MTHD is a recently-

developed hysteretic damper with a controllable post-elastic stiffness. To keep the dampers from being activated during the thermal displacements, the attachment of the dampers to the deck is made through elongated holes oriented in the longitudinal direction of the bridge. The size of these gaps depend on the amount of expected maximum thermal displacement in each pier and is thus different for different piers. This means that the number of the dampers to be engaged during an earthquake will depend on the intensity of the displacements. The slotted connections of MTHD ensures a progressive energy dissipation that is a function of the intensity of the earthquake in the longitudinal direction where the piers are weaker. The progressive design solution ensures minimal or no damage of substructure at small intensity, more frequent earthquakes while damage progressively increases in response to less frequent, larger earthquakes. The progressive / adaptive solution used in the design balanced the damage and risk producing an economical design solution.

REFERENCES

[1] M. Dicleli, "Performance of seismic-isolated bridges with and without elastic-gap devices in near-fault zones," Earthquake Engineering and Structural Dynamics, vol. 37, Issue 6, pp. 935-954, 2008.

[2] Rawlinson, T. A., Marshall, J. D., Ryan, K. L., and Zargar, H. "Development and experimental evaluation of a passive gap damper device to prevent pounding in base-isolated structures" Earthquake Engineering and Structural Dynamics, 44: 1661–1675, 2015.

[3] Zargar, H., Ryan, K. L., Rawlinson, T. A., and Marshall, J. D. "Evaluation of a passive gap damper to control displacements in a shaking test of a seismically isolated three-story frame" Earthquake Engineering and Structural Dynamics, 46: 51–71, 2017.

[4] K. Ö. Çetin, *Probabilistic seismic hazard analysis of Bitlis River Viaduct*, Technical Report, Middle East Technical University, METU Revolving funds Project No. 2010.03.03.01.03.24, Ankara, Turkey, 2010 (in Turkish).

[5] Makris N. and Chang S. *Effect of damping mechanisms on the response of seismically isolated structures*, PEER Report 1998/06. Pacific Earthquake Engineering Research Center, University of California, Berkeley, 1998.

[6] Salem Milani, A., and Dicleli, M. "Systematic development of a new hysteretic damper based on torsional yielding: part I—design and development", Earthquake Engineering and Structural Dynamics, vol. 45, issue 6, pp. 845–867, 2016.

[7] Salem Milani, A., and Dicleli, M. "Systematic development of a new hysteretic damper based on torsional yielding: part II—experimental phase", Earthquake Engineering and Structural Dynamics, vol. 45, issue 5, pp. 779–796, 2016.

[8] Hindi R. A. and Sexsmith R. G. "A proposed damage for RC bridge columns under cyclic loading", Earthquake Spectra, vol. 17, no. 2, pp. 261–289, 2001.